16

Order by Disorder and Topology in Frustrated Magnetic Systems

E.F. Shender and P.C.W. Holdsworth

ABSTRACT The phenomenon of order by disorder in frustrated magnetic systems is reviewed. Thermal, quantum, and even quenched noise may sometimes increase ordering in systems where energetics ensure a nontrivially degenerate classical ground state. In systems where the number of variables parametrizing the manifold of degenerate ground states is not macroscopic, fluctuations may remove the degeneracy and reduce the symmetry to that of the Ising model. We concentrate on the kagomé antiferromagnet, whose manifold of ground states has a macroscopic number of degrees of freedom. In this system, thermal fluctuations around ground states lead to entropically driven local spin nematic order at low T. The fluctuations are so strong that no single state or finite set of states is selected. We derive an effective Hamiltonian, giving a description in terms of the variables of a fluctuating surface. A novel phenomenon, that of quasi-nonergodicity, arising in a perfectly frustrated lattice, is briefly discussed.

16.1 Introduction

In condensed matter physics, it is usual that fluctuations, whether thermal or quantum, suppress order in the system in question. This is not, however, a rigorous rule. In this chapter, we consider a class of magnetic systems where order is induced—or at least the tendency to be ordered is increased—by fluctuations.

In a "conventional" many-body system, the classical energy at zero temperature has a unique minimum for a state with long-range order (global degeneracies, such as the continuous rotations in the Heisenberg or XY models, or the "up" and "down" degeneracy of the Ising model not included). All fluctuations, whether thermal, quantum, or spatial fluctuations of the interparticle couplings, may lead only to a suppression of the order.

The situation is quite different if the classical ground state of a macroscopic system is infinitely degenerate rather than unique. Such a property is a consequence of the special geometry of some lattices. Probably the simplest example is the Ising antiferromagnet on the triangular lattice. Considering a single triangle of spins, one sees that after fixing the direction of one spin to remove the global up–down degeneracy, a twofold degeneracy remains. Thus, a ground state degeneracy arises as the system is unable to simultaneously satisfy the minimum energy condition for all bonds in the system—the phenomenon known as "frustration."

M. Millonas (ed.), *Fluctuations and Order*

A number of frustrated magnetic lattices are known for the Ising and rotationally invariant Hamiltonians. The classical Heisenberg systems are characterized by continuously degenerate ground states. These states form a surface in phase space parametrized by a set of continuous variables, which we refer to as the *ground state manifold.* The possibility of the system wandering over the ground state manifold without crossing any energy barriers, that is, the possibility of going from one ground state to another by a continuous change of variables, results in modes in the excitation spectrum at zero energy—the so-called zero modes. It is intuitively clear that the larger the number of zero modes, the easier it will be for the system to fluctuate and that the number of zero modes must depend on the dimension of the ground state manifold. As we will see, the most interesting cases are where the manifold is "macroscopically degenerate," that is, where the manifold has a dimension of order N, the number of spins. Such systems can be called strongly fluctuating, and it is natural to expect them to exhibit new types of cooperative behavior. No perturbation analysis of these systems is possible, as there are zeros in the denominators of the expansion, and every term in the series is divergent. The source of strong fluctuations is not related to the special properties of low-dimensional systems, despite the fact that some of the best examples are two-dimensional. It is rather the degeneracy of the ground state manifold that is the relevant factor.

Fluctuations have a special role in these systems because they may partially lift the degeneracy and so make systems more ordered: The principal effect of frustration is to ensure that the classical ground state manifold is of higher symmetry than the underlying Hamiltonian. Quantum or thermal fluctuations can dynamically break this additional symmetry, restoring that of the Hamiltonian. For the classical Ising systems, the effect, called "order by disorder," has been proposed by Villian et al. [1], while order by quantum disorder was first considered by Shender [2].

The structure of this chapter is as follows: In Secs. 16.2 and 16.3 we consider order by disorder in systems where the number of zero modes, n_0, is finite, or even infinite, but not macroscopic, that is, $n_0 = N^\alpha$, with $\alpha < 1$. In Secs. 16.4 to 16.6, we discuss the much more interesting case of a system with a macroscopically degenerate ground state manifold. The kagomé and pyrochlore antiferromagnets are examples of such strongly fluctuating systems, which are under intensive theoretical and experimental investigation at present. We show how, in the classical limit, order by disorder works to select from the manifold of possible states a subset of states that maximizes the number of zero modes. In the kagomé antiferromagnet, this subset of states has nematic spin behavior. We present a topological mapping of the ground states for the kagomé system and derive an effective Hamiltonian to represent it as a type of membrane problem. In this way, we are able to describe such systems in terms of the physics of fluctuating surfaces.

Glassy behavior is observed in real kagomé and pyrochlore systems by performing "field cooled" and "zero field cooled" experiments [3, 4]. However there is some evidence, both experimental [3, 4] and theoretical [5], that this behavior is not due to the presence of defects, as is the case in spin glasses [6]. Rather, it seems

to be due to the properties of the uniformly frustrated pure system. Nonergodic behavior is observed in numerical simulations of the pure, undiluted kagomé lattice [7, 8], for which the term *entropy glass* [8] is appropriate. In Sec. 16.4, we discuss the relevance of this novel kind of nonergodicity to experimental observations.

This is by no means a complete review of the field. We restrict ourselves to Heisenberg spin systems, presenting the main ideas and results only, and do not discuss specific systems under experimental study. Those interested in systems with Ising symmetry may look at Liebermann [9] and Leibowitz et al. [10] and references therein.

16.2 Order by Disorder in a Heisenberg Magnet With One Additional Zero Mode ($n_0 = 1$)

16.2.1 Order by Quantum Disorder

Let us consider a Heisenberg antiferromagnet on a body-centered cubic (bcc) lattice, with short-range exchange. We consider only nearest neighbor (NN) couplings, J_1, and next nearest neighbor (NNN) couplings, J_2, and take the NNN coupling to be antiferromagnetic, i.e., $J_2 > 0$. The bcc lattice can be considered as two interpenetrating simple cubic (sc) subsystems coupled by the parameter J_1. Without any magnetocrystalline anisotropy, the Hamiltonian is

$$H = J_1 \sum_{<i,j>} \mathbf{S}_{1i}.\mathbf{S}_{2j} + J_2 \sum_{<p=1,2;i,j>} \mathbf{S}_{pi}.\mathbf{S}_{pj}, \tag{16.1}$$

where S_{1i} and S_{2i} are spins from the first and second subsystems, respectively. The classical ground state of the system for a ratio $|J_1|/J_2$ not too large is presented in Fig. 16.1. This is the so-called "second kind" ordering in the bcc lattice. The structure can be considered as two interpenetrating sc antiferromagnetic subsystems. The local field of one subsystem on the other vanishes, leaving them disconnected and giving a degeneracy additional to the global Heisenberg rotational invariance.

The additional degeneracy has consequences for the excitation spectrum of the system. For an arbitrary angle between spin directions in the subsystems, the classical Landau-Lifshitz equations of motion (or the quantum equations of motion in the limit of infinite S and finite value of energy JS^2) lead us to an excitation spectrum consisting of two acoustic branches, each with a zero mode at $q = 0$. The Goldstone, or zero energy, mode of one of these branches is due to the global Heisenberg invariance, while the second branch, which may be called the *phason*, corresponds at zero momentum ($q = 0$) to the out-of-phase rotation of spins in different subsystems. The absence of a gap is a consequence of the additional degeneracy of the ground state structure considered earlier [2]. Thus, in the classical treatment we have a one-dimensional manifold of ground states, with one zero energy mode coming from the phason branch at $q = 0$.

The phason mode is a true zero mode, in that the energy of rotation is zero to all orders of perturbation, not just in the harmonic approximation. In Sec. 16.4, we

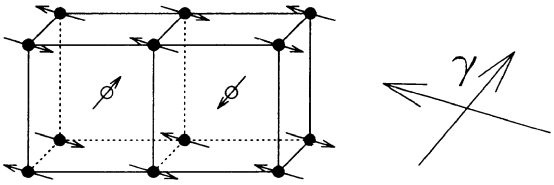

FIGURE 16.1. Second kind of antiferromagnetic ordering on a bcc lattice. Open and closed circles represent sites on the two subsystems. The angle γ between staggered magnetizations of the two subsystems is shown in the inset.

encounter modes that are of zero energy in the harmonic approximation but are of nonzero energy in a higher order calculation.

As is well known, for a real antiferromagnetic system, the classical approach is never rigorous, and quantum effects must be taken into account. The staggered magnetization is

$$\mathbf{M}_p = \frac{1}{N_p} \sum_{<i=1,N_p>} < \mathbf{S}_{pi} > u_{pi}, \tag{16.2}$$

where N_p is the number of spins in subsystem p, and u_{pi} is a staggered variable with values ± 1 corresponding to the two Néel sublattices of the subsystem p. $\mathbf{M}_p$ does not commute with the Heisenberg Hamiltonian, which results in zero point motion around the classical Néel ground state. If the J_1 coupling is small compared to J_2, it does not influence the quantum spin fluctuations within a subsystem very much, but it does result in a coupling of the fluctuations in different subsystems [2]. Although small, the energy of the coupling, E_{quant}, is important because it depends on γ, the angle between the staggered magnetizations $\mathbf{M}_1$ and $\mathbf{M}_2$ (see Fig. 16.1).

$$E_{quant} \sim -(1 + \cos^2(\gamma)) J_1^2 S / J_2. \tag{16.3}$$

It is easy to explain this result qualitatively in the limit of large S. To lowest order in $1/S$, only quantum spin fluctuations of the components perpendicular to the staggered magnetization exist. Choosing a coordinate system with the z axes directed along $\mathbf{M}_1$, and with $\mathbf{M}_2$ in the x–z plane, we see that the interaction of the y components of spin is independent of γ, while that between the x components introduces a coupling between the two subsystems dependent on γ, as $S_{2x} \sim \cos(\gamma)$. There is no contribution from $S_{1x} S_{2x}$ if $\gamma = \pi/2$, so E_{quant} has twice the magnitude for $\gamma = 0$ as for $\gamma = \pi/2$, in agreement with Eq. (16.3). This energy, E_{quant}, is of the form of an effective biquadratic coupling between spins in the different subsystems and makes them collinear. Hence, the continuous rotational phason symmetry becomes broken by fluctuations and is replaced by Ising symmetry; that is, the fluctuations make the system more ordered.

Another way to treat the phenomenon is to represent the energy as

$$E = E_{gs} + \frac{1}{2} \sum_{<n,k>} \hbar\omega_n(k), \tag{16.4}$$

where E_{gs} is the energy of the classical ground state, and $\omega_n(k)$ is the spin wave frequency at wave vector k, with branch index n. The system selects the state that minimizes the sum over spin wave energies, which, in turn, depends on γ. The softest state is selected by fluctuations, and the two subsystems become aligned. Using the spin wave approach, one can calculate E_{quant} rather accurately over the whole region of stability of order of the second kind, not just for small values of $|J_1|/J_2$.

Lifting the phason degeneracy induces a gap in the phason branch [2]. This quantum exchange gap has been detected by inelastic neutron scattering [11].

Order by quantum disorder is very general in that it should exist in any quantum system with classically degenerate ground states. Perturbation arguments show that the quantum fluctuations select the softest state (or states), which provides the minimum energy. This conclusion has been confirmed by studies of different quantum spin systems (see [12, 13, 14, 15] and references therein).

16.3 Order by Thermal Fluctuations

At nonzero temperatures, thermal fluctuations contribute to the effective interaction, as in Eq. (16.3). This contribution cannot be neglected at temperatures close to the Néel temperature T_N, and it has been shown that it is necessary to take this effect into account to explain the stability of structures and T_N values of some antiferromagnetic garnets [2, 16].

In the classical limit, the energy E_{quant} vanishes, and there is only thermal noise in the system. Villain [1], considering an Ising system, first showed that thermal fluctuations can lead to selection of preferred states in this limit. Henley [17] showed, using systems on face-centered cubic (fcc) and bcc lattices, that order by thermal disorder can make some states preferable in classical Heisenberg antiferromagnets. From this, one can see that thermal fluctuations in the classical system stabilize the same collinear spin state as in the quantum case at $T = 0$.

16.4 Systems With More Than One Zero Mode

The Heisenberg antiferromagnet on an fcc lattice consists of four interpenetrating sc lattices. Suppose again that the interaction J_2 within subsystems is antiferromagnetic and is much larger than the interaction $|J_1|$ between nearest neighbors on different subsystems. In the classical ground state, or in the mean field approximation, these four antiferromagnetic subsystems are decoupled from one another, and

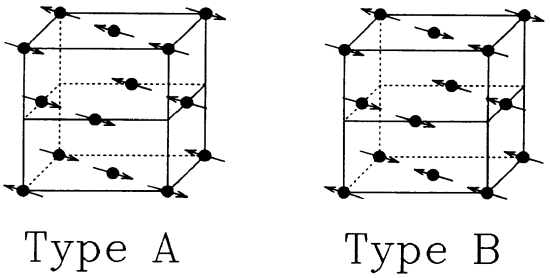

FIGURE 16.2. Type A and type B structures for second-kind antiferromagnetic ordering on an fcc lattice.

five independent variables are required to describe the ground state manifold. The excitation spectrum now consists of four acoustic branches, with three new true zero modes at $q = 0, n_0 = 3$, corresponding to three phason-like sublattice modes. The effective biquadratic exchange interaction found in [2] again forces all spins to be collinear, but it does not fix the relative orientation of the four subsystems. To determine this, Yildirim et al. [18] introduced Ising variables σ_i to describe the spin orientation on the ith subsystem, relative to subsystem 1. Symmetry considerations show that the four subsystems can be arranged in only two different ways, A and B, as shown in Fig. 16.2. In arrangement $A(B)$ the product of the four spins on each tetrahedron of nearest neighbors is positive (negative). Quantum fluctuations give rise to an effective interaction $K_4(\sigma_i)$, the sign of which favors the arrangement A with spins ferromagnetic in [111] planes and antiferromagnetic from plane to plane. The magnitude of K_4 is of order $(|J_1|/J_2)^4$, which indicates that this interaction arises from simultaneous fluctuations of the four subsystems.

As an example of a system with an infinite number of subsystems, we consider the body-centered tetragonal antiferromagnet, in which there are dominant antiferromagnetic interactions, J_2, between spins in the same quadratic layer and much weaker interactions, J_1, between nearest neighboring spins in adjacent layers (this case has some relevance for the lamellar copper oxides exhibiting high-temperature superconductivity). In the mean field approximation, every layer is a subsystem decoupled from all others, so the number of zero modes is proportional to the number of layers $(= N^{1/3})$ in the system. The effective biquadratic interaction indicates that the spins will all be collinear. To treat the next level of selection by order by disorder, the nth layer can then be characterized by the Ising variable σ_n, defining the phase of its staggered moment. Symmetry forbids a term of the form $\sigma_n\sigma_{(n+1)}$ in any effective interaction between planes; thus one might expect a random sequencing of antiferromagnetic layers. However, Yildirim et al. [18] showed that quantum fluctuations produce an antiferromagnetic interaction, $K_{eff}\sigma_n\sigma_{(n+2)}$, between alternate layers, where K_{eff} is the effective coupling, found to be of or-

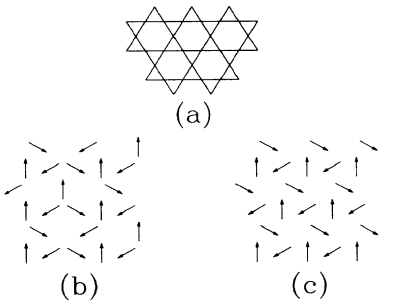

FIGURE 16.3. (a) The kagomé lattice. (b) The $\sqrt{3} \times \sqrt{3}$ ground state. (c) The $q = 0$ ground state.

der $(|J_1|/J_2)^6$. Thus, all couplings allowed by the Hamiltonian symmetry occur if fluctuations are taken into account.

16.5 A System With a Macroscopic Number of Zero Modes: The Classical Kagomé Antiferromagnet

16.5.1 Ground State Manifold and Spin Origami

The nearest neighbor Heisenberg antiferromagnet on the loosely connected kagomé lattice, shown in Fig. 16.3a, is probably the simplest example of a system with a macroscopic number of zero modes. The Hamiltonian for the classical system may be written as the sum over triangles Δ

$$H = J \sum_{<i,j>} \mathbf{S}_i . \mathbf{S}_j = \frac{J}{2} \sum_{<\Delta>} (\mathbf{S}_{1\Delta} + \mathbf{S}_{2\Delta} + \mathbf{S}_{3\Delta})^2 - NJ, \qquad (16.5)$$

where $J > 0$ is the coupling constant and $\mathbf{S}_{i\Delta}$ is a spin of unit length in triangle Δ.

All ground states satisfy the requirement that the vector sum of spins over any triangle must be zero, leaving the three spins lying in a single plane with an angle of 120° between each pair of spins. It is convenient to define the direction of the spin plane for each triangle by a unit vector perpendicular to its surface

$$\mathbf{n}_\Delta = (2/3\sqrt{3})(\mathbf{S}_{1\Delta} \times \mathbf{S}_{2\Delta} + \mathbf{S}_{2\Delta} \times \mathbf{S}_{3\Delta} + \mathbf{S}_{3\Delta} \times \mathbf{S}_{1\Delta}), \qquad (16.6)$$

with spins taken in a clockwise direction around the triangle. The special symmetry of the kagomé lattice means that there is a continuous degeneracy of such ground states, involving local rotations of microscopic numbers of spins. The origin of the

degeneracy is closely connected with the lines of defects, which may be created in a coplanar state and may be understood by considering the two magnetically ordered states shown in Figs. 16.3b and c. These are just two of the special subset of coplanar ground states with all the spins lying in the same plane and the $\mathbf{n}_\Delta$ vectors lying parallel or antiparallel to each other. The simplest nonplanar state can be generated from the $\sqrt{3} \times \sqrt{3}$ state by rotating a "weathervane defect": each triangle consists of a triad of spins A, B, C, and circling a hexagon one finds spins $A - B - A - B - A - B$, for example, which can be rotated at a cost of zero energy about the spin direction C. Rotating the spins through 180° leads to a new coplanar state with defects in the magnetic order. Disordered coplanar states are characterized by longer sequences of neighboring spins, $A-B-A-B\ldots$, interior to the line of spins C, giving longer line defects. The $q = 0$ state has infinitely long line defects spanning the whole system. Starting from the $\sqrt{3} \times \sqrt{3}$ state, any nonplanar ground state and any one of the a^N coplanar states, where $a \sim O(1)$ [19] can be reached by rotating a series of line defects.

Together with Cherepenov and Berlinsky, we recently presented a way of visualizing geometrically the ground state manifold by mapping the spin planes of each triangle onto a membrane surface [5]. A spin triad from a triangle of the kagomé lattice may be represented in spin space as a closed equilateral triangle (Fig. 16.4a). In this way, five spins which belong to two adjoining kagomé lattice triangles, may be represented by two coplanar triangles sharing the edge that corresponds to the spin on the shared site. The relative orientation of the spin planes of the two triangles is given by the vectors $\mathbf{n}_\Delta$ defined earlier. For the $q = 0$ planar state the $\mathbf{n}_\Delta$s are all parallel, and the spin surface maps onto a macroscopic triangular lattice (Fig. 16.4b), while in the $\sqrt{3} \times \sqrt{3}$ state, the Néel order of the $\mathbf{n}_\Delta$ vectors means that alternate triangles are superposed on top of each other, and the whole spin surface folds onto a single elementary triangle (Fig. 16.4c). The ground state manifold is now represented by the configuration space of the spin membrane with undistorted triangles, and the line defects are folds in the membrane surface. Crumpled and buckled surfaces correspond to nonplanar ground states. We call this folding of the spin surface *spin origami* [5], a term first introduced by Chandra et al. [8], who considered the folding of line defects of large length scale.

This mapping shows that the physics of the kagomé system is related to that of membranes, or fluctuating surfaces (see [5] and [20]); we return to the mapping later.

16.6 Selection of Coplanar States by Order by Disorder

In this section, we show that order by disorder works, at small but finite temperature, to select from the ground state manifold the subset of coplanar states. First, one must calculate the excitation spectrum above the ground state for different points on the manifold. Zeng and Elser [21] showed, by numerical analysis of the spin wave equations of motion, that at least some ground state configurations have a complete branch of zero energy excitations. That is, a branch with zero modes,

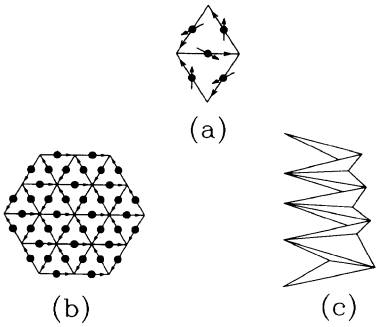

FIGURE 16.4. Spin origami: The spins of each triangle are mapped onto a triangular surface in spin space. (a) Five adjoining spins forming two triangles sharing a single edge. The relative orientation of the two triangles is given by the $\mathbf{n}_\Delta$ vectors (Eq. (16.6)). For the planar state shown, this reduces to the direction of circulation around the edges of an origami triangle. (b) Section of the $q = 0$ state; the circulation is in the same direction for all triangles, and the mapping gives an extensive surface in spin space. (c) Section of the $\sqrt{3} \times \sqrt{3}$ state; here the circulation is in the opposite direction for "up" and for "down" triangles, and the spin surface folds onto a single origami triangle.

not just at $q = 0$, but for all values of q. In the work of Chalker and the present authors [7], we calculated the classical excitation spectrum for an arbitrary coplanar state. Using a local right-handed coordinate system with $\hat{\mathbf{z}}_i$ parallel to $\mathbf{S}_{i\Delta}$, and $\hat{\mathbf{y}}_i$ perpendicular, but in the spin plane, we find the same harmonic Hamiltonian for any coplanar state

$$H_2 = (J/2)[(3\delta_{ij} - M_{ij})\epsilon_i^x \epsilon_j^x + 2M_{ij}\epsilon_i^y \epsilon_j^y]. \tag{16.7}$$

The spin orientations are paramatrized by $\mathbf{S}_i = (\epsilon_i^x, \epsilon_i^y, 1 - \alpha_i)$, with α_i determined from $|\mathbf{S}_i| = 1$. A summation convention is used to define the matrix $\mathbf{M}$: $M_{ii} = 1$; $M_{ij} = \frac{1}{2}$ if i, j are nearest neighbor sites; $M_{ij} = 0$ otherwise. One of the eigenvalues of Eq. (16.7) turns out to be zero over the entire Brillouin zone, giving a complete branch of $N/3$ zero modes, in the harmonic approximation, for any coplanar state. This result has also been obtained for the $q = 0$ and $\sqrt{3} \times \sqrt{3}$ states by Harris et al. [22]. The same is not true of nonplanar states, and we proposed elsewhere [7] that any nonplanar state has fewer zero modes than a coplanar state.

Using the mode-counting arguments of Chalker et al. [7], it is possible to estimate the statistical weights, in the partition function Z, of the phase space around different ground states. First we note that the zero modes in this problem are only excitations at zero energy in the harmonic approximation. Higher-order corrections give an effective quartic potential, and the zero modes are strictly quartic modes. A quartic mode gives a contribution of $(T/J)^{1/4}$ to the classical partition function Z, while quadratic modes give a contribution $(T/J)^{1/2}$. For a small re-

gion of phase space containing a ground state characterized by N_4 quartic, and N_2 regular quadratic modes, Z is of the form

$$Z = A\left(\frac{T}{J}\right)^{\left(\frac{N_4}{4}+\frac{N_2}{2}\right)}, A = a^N, \tag{16.8}$$

with a a constant of order unity. The partial free energy of the region of phase space near different ground states, which we define $f = -T\ln(Z)$, is

$$f = -TN\ln(a) - T\left(\frac{N_4}{4}+\frac{N_2}{2}\right)\ln\left(\frac{T}{J}\right). \tag{16.9}$$

It is clear that, in the limit $T \to 0$, the system can maximize the partition function and minimize the partial free energy for such a region of phase space if it approaches one of the states with the maximum number of zero modes. We therefore conjectured [7] that the system should select from the manifold of states the subset of coplanar states, as it is these states that have the maximum number of zero modes. We confirmed this conjecture by Monte Carlo simulation [7]. We see the buildup of nematic correlations in the $\mathbf{n}_\Delta$ vectors. The correlation function $g(r)$ is defined

$$g(r) = \left(\frac{3}{2N_r}\sum_{|\mathbf{r}_\alpha-\mathbf{r}_\beta|=r}\langle(\mathbf{n}_\alpha.\mathbf{n}_\beta)^2\rangle - \frac{1}{2}\right), \tag{16.10}$$

where the brackets $\langle..\rangle$ indicate a thermal average, and the sum is over the N_r pairs of triangles α and β, with $|\mathbf{r}_\alpha-\mathbf{r}_\beta| = r$. $g(r)$ becomes nonzero over the system sizes studied, for $T/J < 0.01$, and tends to unity in the limit $T \to 0$. The presence of quartic modes is also evident in the specific heat. Classical equipartition of energy gives a contribution of $1/2k_B$ to the specific heat for each quadratic mode, and $1/4k_B$ for each quartic mode, where k_B is Boltzmann's constant. In total, for the N spins with Heisenberg interactions, there are $2N$ modes, $N/3$ of which are quartic. The specific heat per spin is therefore $C_v/Nk_B = 11/12$ rather than unity. Comprehensive simulation results for other thermodynamic quantities are given by Huse and Rutenberg [23] and Reimers and Berlinsky [24].

From Eq. (16.9), we see that the difference in partial free energy between two coplanar states that are distant in phase space is $\sim NT$, while if two states have numbers of zero modes differing by ΔN_4, their free energies differ by the change in this number, $\Delta f \sim \Delta N_4 T\ln(T/J)$. Spin origami is a useful tool for visualizing this change. Starting from a coplanar state, if we rotate a line defect, this corresponds to making a fold in the planar spin surface. If the line defect is rotated away from the planar region, N_4 will decrease by the number of hexagons touching the fold, as the quartic modes associated with these hexagons will become quadratic. The change in free energy is then $\Delta f \sim LT\ln(T/J)$ [8], where L is the length of the line defect. In a typical nonplanar state represented, in spin origami, by a substantially crumpled surface, the number of zero modes will be much less than for a planar state, with the probable result $\Delta N_4 = N/3 - N_4 \sim N$.

One can understand from this folding why long equilibration times are observed in simulations for coplanar states with long line defects [7, 24]. In traversing between two coplanar states via a nonplanar, or crumpled, state, the system must traverse large free energy barriers, which may be of order L and will lead to nonergodicity. The term *entropy glass*, introduced by Chandra et al. [8], therefore seems a very suitable one to describe the system.

The considerations of this section do not allow us to determine which one of the coplanar states has maximum probability. Harris et al. [22] derived the momentum-dependent magnetic susceptibility from a high-temperature expansion and concluded that it is maximal for the $\sqrt{3} \times \sqrt{3}$ state, indicating that its statistical weight is the biggest. One might think that this should result in its ultimate selection, and the development of a staggered magnetic moment corresponding to $\sqrt{3} \times \sqrt{3}$ order in the limit $T \to 0$. This is the conclusion of the self-consistent treatment of Chubukov [25], and in Huse and Rutenberg [23], Monte Carlo data are extrapolated to the limit $T \to 0$ to give evidence of such a moment. However, it would remain unsaturated (i.e., < 1), and it is clear that fluctuations remain right to the limit $T \to 0$. In the next section, we examine the strongly fluctuating nature of the system and show that the question of long-range order is far from resolved. We present arguments that suggest there should, in fact, be no development of magnetic order as $T \to 0$.

16.7 Does the Question "What Particular Coplanar State Is Selected?" Make Sense?

In the Monte Carlo study of Reimers and Berlinsky [24], they show a snapshot of a well-relaxed low-temperature state. The snapshot clearly does not show evidence of the ultimate selection of the $\sqrt{3} \times \sqrt{3}$ state; rather, it shows a composition of different $\sqrt{3} \times \sqrt{3}$ domains. It is simple to produce such domains, starting from the $\sqrt{3} \times \sqrt{3}$ state and flipping weathervane defects and more complicated spin clusters. In three possible weathervane defects, spins AB, BC, or AC are rotated.

This result can be understood by estimating the free energy cost of creating a domain wall in the $\sqrt{3} \times \sqrt{3}$ state. From the preceding counting modes argument, the difference in free energy between the two coplanar states is in the constant A, defined in Eq. (16.8), and the only difference here must be from the contribution of the spins along the line defect, or domain wall. If the length of the wall is L, we may write

$$A_1 = {a_1}^N, A_2 \sim {a_1}^{N-L} {a_2}^L, \tag{16.11}$$

where A_1 and a_1 are constants related to the $\sqrt{3} \times \sqrt{3}$ state, and A_2 and a_2 to the domain state. The difference in free energy between the two states is therefore $\Delta f \sim LT$.

If we consider a state that is a set of domains of typical length L of the order of several lattice spacings, then there are a macroscopic number of line defects with total cost in free energy of order NT. The probability of having one such

state would be smaller than that for the $\sqrt{3} \times \sqrt{3}$ state by a factor $\exp(-\alpha N)$, where α is a numerical factor. However, the number of possible states of this kind is of order $(\eta N!)$, where η is a different numerical factor, which suggests that the ensemble of domain states should be preferred over the $\sqrt{3} \times \sqrt{3}$ state. Of course, the real situation is somewhat more complicated because there are states with a distribution of domain size L (see Ref. [8]) whose distribution function $P(L)$ falls off with L very slowly, $P(L) \sim L^{-2/3}$, but these can only increase the weight of the nonmagnetic states, relative to the $\sqrt{3} \times \sqrt{3}$ state. These rough arguments, involving the smallest domain sizes only, explain the domain structure observed in Monte Carlo snapshots, and we believe they incorporate the essential physics involved. No large domains of either the $q = 0$ state, or of other states characterized by different configurations of the spin triad making up the coplanar state, were observed by Reimers and Berlinsky [24]. The only evidence of different structures was the observation of one very small domain of the $q = 0$ state [26]. This is probably because the coefficient a that characterizes them is somewhat smaller, with the result that they occur with too small a probability to be observed in the small system sizes studied.

If we consider the statistical weight as a function over the subspace of coplanar states, it will have a maximum for the $\sqrt{3} \times \sqrt{3}$ state. However, the maximum will be very flat, and the system will not spend much time in this state. The picture that emerges means that the classical kagomé antiferromagnet really is a strongly fluctuating system. We therefore cannot restrict ourselves to the $\sqrt{3} \times \sqrt{3}$ state and states close to it when we calculate the partition function. Neither can we take into account only a finite number of coplanar states. In this sense, the question "What state is selected by fluctuations?", given very often in the beginning of the study of these systems, has no sense.

16.8 An Effective Hamiltonian and Description as a Fluctuating Surface

The part of phase space that we have to take into account to describe the system consists of all coplanar states and states slightly distorted from them. For the zero modes, or in the soft zone, the anharmonic forces cannot be ignored, as we have discussed. These describe the interaction of zero modes with the conventional spin waves [7],

$$H_3 = (J/2) \sum_{\langle i,j \rangle} \hat{\mathbf{x}}_i . \hat{\mathbf{z}}_j (\epsilon_i^{y2} \epsilon_j^x - \epsilon_j^{y2} \epsilon_i^x), \tag{16.12}$$

and the interaction between the zero modes themselves [7],

$$H_4 = (J/16) \sum_{\langle i,j \rangle} (\epsilon_i^{y2} - \epsilon_j^{y2})^2. \tag{16.13}$$

The product $\hat{\mathbf{x}}_i . \hat{\mathbf{z}}_j$ in Eq. (16.12) has a very simple interpretation; it is proportional to the chirality of the pair of spins, $\sigma_{i,j}$, defined as $+1(-1)$ if spin $\mathbf{S}_i$ must be rotated

clockwise (anticlockwise) to lie in the direction of $\mathbf{S}_j$, giving $\hat{\mathbf{x}}_i.\hat{\mathbf{z}}_j = \sqrt{3}/2(\sigma_{i,j})$.

It is interesting that H_4, like H_2, is independent of the coplanar state that is being considered, while H_3, because of the coefficient $\hat{\mathbf{x}}_i.\hat{\mathbf{z}}_j$, is state dependent (see also Ref. [25]). The Hamiltonian H_3 contains the interaction of two zero modes with the spin wave modes associated with ϵ_x. There is no interaction, in H_3, between the zero modes, as no term proportional to ${\epsilon_y}^3$ is possible because of symmetry reasons. In H_4, terms of the form ${\epsilon_x}^2{\epsilon_y}^2$ are omitted, as they are not relevant.

To obtain an effective zero modes Hamiltonian, we will integrate over the fast motion, that is, over spin wave degrees of freedom. In order to do this, we must diagonalize H_2, as done by Chalker et al. [7] and Harris et al. [22]. Once in Fourier space, the spin wave part of H_2 is diagonalized by the linear transformation

$$ {\epsilon^x}_\mu(\mathbf{k}) = \sum_{\alpha=1}^{3} C_{\mu\alpha}(\mathbf{k}) E_\alpha(\mathbf{k}), \tag{16.14} $$

where indices $\mu = 1, 2, 3$ are for the three sites in the kagomé lattice unit cell with coordinates $r_1 = (a, 0), r_2 = (a/2, -\sqrt{3a/2}), and r_3 = (0, 0)$. Values of the eigenvalues and eigenvectors may be easily obtained [7, 22]:

$$ \lambda_1 = 3, \lambda_{2,3} = \frac{3}{2} \pm \frac{1}{2}\sqrt{4(\cos^2(k_1) + \cos^2(k_2) + \cos^2(k_3)) - 3}, \tag{16.15} $$

$$ \mathbf{C}_{mu} = \begin{pmatrix} C_{\mu 1} \\ C_{\mu 2} \\ C_{\mu 3} \end{pmatrix} = \frac{1}{N_\mu} \begin{pmatrix} \cos(k_1)\cos(k_{12}) + (2 - \lambda\mu)\cos(k_{12}) \\ (2 - \lambda\mu)^2 + \cos^2(k_1) \\ \cos^2(k_1)\cos^2(k_{12}) + (2 - \lambda\mu)\cos(k_2) \end{pmatrix}, \tag{16.16} $$

where $k_1 = k_x a, k_2 = (k_x a - \sqrt{3}k_y a)/2, k_{12} = k_1 a - k_2 a$ and the normalizing factors N_μ are

$$ \begin{aligned} N_1 &= \sin(k_1)\sqrt{2(1 - \cos(k_1)\cos(k_2)\cos(k_{12})} \\ N_2 &= \left(\lambda_3{}^2(k)(1 + \cos^2(k_{12}) + \cos^2(k_2)) - {N_1}^2\right)^{1/2} \\ N_3 &= \left(\lambda_2{}^2(k)(1 + \cos^2(k_{12}) + \cos^2(k_2)) - {N_1}^2\right)^{1/2} \end{aligned} \tag{16.17} $$

Integrating $\exp(-\beta(H_2 + H_3 + H_4))$ over all ϵ_x and the ϵ_y not associated with the zero modes, we get the following effective Hamiltonian:

$$ \begin{aligned} H_{eff} &= H_4 + \tilde{H}_{eff} \\ \tilde{H}_{eff} &= -\frac{J}{8} \sum_{\substack{\mathbf{R}_\alpha, \mathbf{R}'_{\alpha'} \\ \rho_\beta, \rho'_{\beta'}}} T^{\alpha'\beta'}\left(\mathbf{R}'_{\alpha'} - \rho'_{\beta'}\right) \\ &\quad \left(\epsilon^y_{\mathbf{R}_\alpha}\right)^2 \left(\epsilon^y_{\rho_\beta}\right)^2 \sigma_{(\mathbf{R}_\alpha, \mathbf{R}'_{\alpha'})} \sigma_{(\rho_\beta, \rho'_{\beta'})}, \end{aligned} \tag{16.18} $$

where the tensor $T^{\alpha'\beta'}(\mathbf{r})$ is

$$ T^{\alpha'\beta'}\left(\mathbf{R}'_{\alpha'} - \rho'_{\beta'}\right) = $$

$$\frac{3}{4} \sum_{\substack{\mu = 1,2,3 \\ \mathbf{k}}} \frac{1}{\lambda_\mu(\mathbf{k})} C_{\mu\alpha'}(\mathbf{k}) C_{\mu\beta'}(\mathbf{k}) \cos(\mathbf{k}.\left(\mathbf{R}'_{\alpha'} - \boldsymbol{\rho}'_{\beta'}\right)). \quad (16.19)$$

$\mathbf{R}_\alpha$, $\mathbf{R}'_{\alpha'}\boldsymbol{\rho}_\beta$, $\boldsymbol{\rho}'_{\beta'}$ run over all the sites of the kagomé lattice, $\mathbf{R}_\alpha = \mathbf{R}+\mathbf{r}_\alpha$, where $\mathbf{R}$ is the coordinate of the unit cell, and $\mathbf{r}_\alpha$ is the coordinate of the site within the cell. Pairs of coordinates for the chirality (e.g., $(\mathbf{R}_\alpha, \mathbf{R}'_{\alpha'})$) are nearest neighbors.

We keep, in Eq. (16.18), only the part of ϵ_y associated with the zero modes.

$$\epsilon^y_{\mathbf{R}\alpha} = \frac{1}{\sqrt{N}} \sum_k \epsilon^y_\alpha(k) e^{-i(\mathbf{k}.\mathbf{R}\alpha)},$$
$$\epsilon^y_\alpha(k) = C_{\alpha 1}(k) E^y_1(\mathbf{k}). \quad (16.20)$$

The calculation of the partition function from the effective Hamiltonian for zero modes presented earlier implies integrating over all continuous variables ϵ_y and summing over all allowed sets of chiral variables σ.

The principal feature of the H_{eff} is the absence of the elastic quadratic term, so fluctuations are even more important than for conventional membranes [27]. It is not surprising that the chiralities interaction, which originates from the third-order coupling of two zero modes and a spin wave mode, turns out to be long ranged. At a large distance between two bonds, the leading contribution to $T^{\alpha'\beta'}(\mathbf{r})$ comes from the term with $\mu = 3$, as $\lambda_3(\mathbf{k}) \sim k^2$ for small $\mathbf{k}$ and provides a power-law-like fall in $T^{\alpha'\beta'}(\mathbf{r})$ with distance.

The Hamiltonian H_{eff} gives a rigorous description of the thermodynamic properties of the classical kagomé antiferromagnet at low T. This puts the classical kagomé antiferromagnet in the class of highly fluctuating surface problems. A self-consistent approximation to this problem would involve decoupling the product of four continuous variables and replacing one of the pairs by an average for a fixed configuration of chiralities. It has been shown [25]—using a technique that, if one started from our H_{eff}, would be equivalent to this decoupling—that the $\sqrt{3} \times \sqrt{3}$ state is selected and that the branch of zero modes is replaced by a temperature-dependent acoustic branch. The neglect of fluctuations means that not enough weight is given to the disordered states that have only a marginally smaller probability and whose sum will have a larger weight than that of the magnetic state.

16.9 Magnetic Field Effects

In the presence of an external magnetic field, h, along the direction $\hat{\mathbf{z}}$, the term

$$-\frac{h}{2} \sum_{\Delta, i=1,2,3} \hat{\mathbf{z}}.\mathbf{S}_{\Delta i} \quad (16.21)$$

is added to the Hamiltonian. The minimum energy condition becomes, for each triangle,

$$J(\mathbf{S}_1 + \mathbf{S}_2 + \mathbf{S}_3) - \frac{h}{2}\hat{\mathbf{z}} = 0. \tag{16.22}$$

This condition may be satisfied for canted states, where the three spins in a triangle no longer lie in a single plane, and for planar states where all spins are coplanar with the magnetic field. There is a continuous degeneracy of spin triads for both the canted and the planar states, which satisfies the minimum energy requirement. In addition, there are an infinite number of ways of distributing any of these triads over the kagomé lattice for any ground state, as in the case of zero field. It is easy to see that there are also states that contain more than three possible spin orientations. These may be obtained from the $\sqrt{3} \times \sqrt{3}$ distribution of a spin triad by rotating, for example, a $\mathbf{S}_1 - \mathbf{S}_2 - \ldots$ hexagon about the axis defined by $\mathbf{S}_3 - \frac{h}{2J}\hat{\mathbf{z}}$. Thus, the magnetic field does not remove the infinite ground states degeneracy unless the field exceeds the value $h_c = 6J$, which makes all spins collinear.

In order to predict which states are entropically selected, we need, as in the zero field case, to identify the states with the maximum number of zero modes. The harmonic analysis shows immediately that all coplanar states have the same soft zone as in the zero field, though the nonzero harmonic modes and anharmonic corrections are field dependent. For the canted states, simple qualitative arguments show that only those with $\sqrt{3} \times \sqrt{3}$ order of the spin triads have the same branch of $N/3$ zero modes [28]. Counting of modes arguments is unable to distinguish between these states. We find numerically that entropic selection of planar order is maintained in the presence of a field, although the tendency to order is weakened by the field. This is because in the presence of a field the minimum energy condition does not imply spin coplanarity for a single spin triad. Rather, the selection of a unique spin plane for each triangle is driven by order by disorder, as well as the coplanar selection for all triangles. This is contrasted with the case of zero field, where the spins of each triangle are confined to a single plane by the minimum energy requirement of the ground state. This is illustrated in Fig. 16.5, where we show the probability distribution function $P(W)$ for the quantity W

$$W = \frac{(\mathbf{S}_1 \times \mathbf{S}_2).\mathbf{S}_3}{|\mathbf{S}_1 \times \mathbf{S}_2|}, \tag{16.23}$$

where $\mathbf{S}_i$ are the spins of a given triangle. $P(W)$ is calculated from all triangles over a Monte Carlo run of 10^7 Monto Carlo steps (MCS) for both $h/J = 1.0$ and the zero field case. In both cases the temperature was $T/J = 0.00025$. In the presence of the field, the distribution has a measurable width, showing the existence of fluctuations out of the plane, while for zero field the distribution is extremely narrow, and the planar condition for each triangle is almost perfectly satisfied.

A magnetic field is the principal experimental tool used to study nonergodicity in magnetic systems. There is, however, a very important difference between the entropy glasses we are considering now and spin glasses. In spin glasses, a

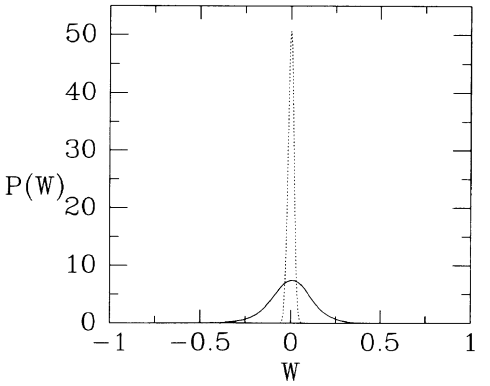

FIGURE 16.5. $P(W)$ versus W for field $h/J = 1.0$ (solid curve) and for zero field (broken curve).

bifurcation is observed in the field cooled (FC) and zero field cooled (ZFC) magnetizations at T_f. This kind of behavior is not possible in the model studied here, as the minimum energy condition (16.22) dictates that all low-energy states must have the same magnetic moment, $M/N = h/6J$. This is confirmed by our Monte Carlo simulations. Thus, states separated by high-entropy barriers have the same magnetization, and no history dependence can occur. Probably a higher-order susceptibility will be sensitive to the freezing history in entropy glasses.

Magnetic measurements performed on the antiferromagnet $SrCr_8Ga_4O_{19}$ [3], which has to a good approximation the kagomé structure, and on some pyrochlore compounds [4], which also have an infinitely degenerate classical ground state structure, demonstrate unambiguously the existence of a bifurcation in the FC and ZFC magnetizations below a freezing temperature T_f. Structural disorder in the pyrochlore system [4] was so small that Gaulin et al. [4] were able to conclude from their neutron scattering and X-ray measurements that the glassy behavior was "intrinsic to the pure pyrochlore magnets." It is difficult to make the same stoichiometric samples of $SrCr_8Ga_4O_{19}$; however, Martinez et al. [3] were able to show that it is very improbable that spatial disorder is the source of the glassy behavior. These results are consistent with theoretical arguments that show that low concentrations of defects do not cause spin glass behavior in pyrochlore [29] and kagomé [5] antiferromagnets.

A possible source of energy barriers and metastable states leading to the bifurcation in the FC and ZFC magnetizations are weak perturbations to the Heisenberg Hamiltonian. For example, an easy plane single ion magnetic anisotropy DS_{iz}^2, $D > 0$ makes coplanar states energetically preferable in zero field and produces energy barriers for transitions from one coplanar state to another. If this results in a bifurcation in the two magnetization curves and a remnant magne-

tization, then the difference between the two curves should disappear when the magnetic field is large enough to depress the energetic structure created by the weak anisotropy. This is exactly what has been seen in the pyrochlore compound [4]. The experimental situation does not exclude easy axis anisotropy $D < 0$, and some results suggest it is present [3]. Numerical work on a kagomé system with easy axis anisotropy shows a rich ground state structure, with an Ising-like magnetic transition [30]. It is not excluded that this energy structure could also lead to bifurcation between the FC and ZFC magnetizations.

From the preceding discussion, it is clear that the field should not change the number of zero modes associated with the preferred states. This is consistent with the recent experimental observation that the specific heat behavior observed in $SrCr_8Ga_4O_{19}$, $C_v \sim T^2$, is not sensitive to the application of a field [3].

16.10 Effect of Spatial Disorder

In a pure frustrated magnetic system, the symmetry allows a high ground state degeneracy. Impurities change the balance of interactions and remove the degeneracies. For example, take the single frustrated triangle of Ising spins considered in Sec. 16.1. If the first spin is fixed, a twofold degeneracy exists because of the two equivalent ways of placing the frustrated bond. If one of the bond stengths is changed, the frustrated bond has a unique preferred position and the degeneracy is lifted. It has been shown that, as long as the number of zero modes is not macroscopic, any finite concentration of defects will remove the degeneracy of the pure system completely [17, 32]. The result of this lifting of degeneracy depends on the symmetry of the perturbation introduced by defects, the space dimension, and the degeneracy manifold [32]. Site disorder results in the selection of one of the states from the initial ground state manifold [17]. Bond disorder may induce an Imry-Ma-type instability [33], leading to a state without any long-range order.

The situation for the pyrochlore and kagomé lattices, where the number of zero modes are macroscopic, is quite different. Using spin origami for the kagomé lattice, we recently demonstrated that for clusters containing not too many impurities we are still able to minimize separately the energy of each triangle, as was the case for the perfect lattice. The discrete spectrum of local spin energies found in simulations by Huber and Ching [34] may be explained immediately by this result. However, impurities necessarily introduce spin canting into the system, as the minimum energy requirement is no longer compatible with the spins being coplanar. The spin canting introduced by an impurity can either be localized, involving only a finite number of spins surrounding the defect, or extended, where the impurity introduces a set of folds spanning the whole system. The free energy, which makes coplanar states more preferable, will favor configurations with localized canting, as this maximizes the coplanar area. We find that for an impurity embedded in a domain of the $\sqrt{3} \times \sqrt{3}$ state, the area of canted spins is the two-hexagon region containing the impurity. This is the minimum canted area; thus, even the minimal number of spins canted out of the spin plane by a nonmagnetic defect is large,

and one would expect nematic order to disappear for a very small concentration of defects. All these results were confirmed by Monte Carlo simulation, where we showed that 2% of impurities is sufficient to remove spin coplanarity almost completely.

The possibility of satisfying spin configurations locally leads to the ground state energy being independent of the configuration of impurities. Therefore, as long as this is true, impurities do not produce conventional spin glass behavior. Above a critical concentration x_c, one can no longer minimize separately finite clusters of spins, and one might then expect the system to behave as a spin glass. Analogous results have been found earlier for the pyrochlore lattice by Villain [29].

16.11 Quantum Kagomé Antiferromagnets

There have been two approaches to the study of the quantum kagomé system. The first is the development of a self-consistent treatment in the quasi-classical limit $S >> 1$. Chubukov [25] and von Delft and Henley [35] assumed that it is possible to divide the phase space of the system into separate parts containing a coplanar state and states slightly noncoplanar but close to the given coplanar state. It was argued that the transition probability, τ, between different coplanar states should be exponential, $\tau = \exp(-S^m)$, where m is a positive and noninteger exponent. This approach leads to the conclusion that the perfect $\sqrt{3} \times \sqrt{3}$ state is stabilized at $T = 0$. The smallness of the transition probability between any pair of coplanar states is not in any doubt, but it seems possible that the large number of states to which the system can tunnel should compensate for this small factor (that is, this would be similar to the contribution given by the large number of domain states in the classical problem). This would lead to the same kind of strongly fluctuating physics that we have discussed for the classical system.

The second avenue of study is that of the $S = 1/2$ kagomé antiferromagnet, which has been stimulated by the studies of ^{3}He films adsorbed onto a graphite surface. No small parameter exists in this problem; that is, $1/S$ cannot be treated as small, and so fluctuations are limitingly strong. It is therefore probably the best candidate for a disordered spin liquid ground state. Results obtained by Elser and collaborators [36], and several other groups [37, 38] are consistent with the existence of such a state.

16.12 Conclusion

The mapping of the kagomé antiferromagnet onto a fluctuating surface problem without an elastic term in the effective Hamiltonian guarantees a difficult time for anyone interested in further developments. In addition to the equilibrium thermodynamics, there are also important dynamical questions. The kagomé antiferro-

magnet has been proposed as a new kind of nonergodic system, an entropy glass, which promises to be an extremely interesting challenge.

Further theoretical and experimental work is required to explain the characteristic bifurcation between the FC and ZFC magnetizations at a temperature T_f, which is observed in experimental kagomé systems. We show, in discussing this point, that it cannot be explained in the framework of the classical Heisenberg model and that relevant weak interactions are required to explain the phenomenon.

Many questions concerning the quantum problem are still wide open. While the $S = 1/2$ quantum system is doubtless one of the best candidates to find a spin liquid state, properties of systems with higher S values are very obscure. $SrCr_8Ga_4O_{19}$, which is proposed as a kagomé antiferromagnet, has $S = 3/2$. It is possible that this system is strongly fluctuating because of the large number of states to which finite spin clusters can tunnel to from the perfect $\sqrt{3} \times \sqrt{3}$ state. No real understanding of the properties of the experimentally studied systems is possible until the behavior of the quantum systems is understood. In this respect, the study of exactly solvable models will be extremely important (see, e.g., Refs. [39, 40]).

16.13 Acknowledgments

It is a pleasure to thank our collaborators for much of the work discussed in this chapter: A.J. Berlinsky, J.T. Chalker, and V.B. Cherepanov. In addition, we are grateful to S.T. Bramwell, M.J.P. Gingras, A.B. Harris, C.L. Henley, and C. Kallin for many useful discussions.

16.14 References

[1] J. Villain, R. Bidaux, J.P. Carton, and R.J. Conte, *J. Phys. (Paris)* **41**, 1263 (1980).

[2] E.F. Shender, *Sov. Phys. JETP* **56**, 178 (1982).

[3] A.P. Ramirez, G.P. Espinisa, and A.S.Cooper, *Phys. Rev. Lett.* **64**, 2070 (1990); G. Broholm, G. Aeppli, G.P. Espinosa, and A.S.Cooper, *Phys. Rev. Let.* **65**, 3137 (1990). F. Martinez, A. Sandiumenge, A. Rouco, J. Labarta, M. Rodrigez-Carvajal, M.I. Tovar, S. Gausa, X. Gali, and S. Obrados, *Phys. Rev. B* **46**, 1078 (1992).

[4] J.E. Greedan, J.N. Reimers, S.L. Penny, and S.V. Stager, *Phys. Rev. B* **43**, 5682 (1991); J.N. Reimers, J.N. Greedan, R.K. Kremer, E. Gmelin, and M.A. Subramanian, *Phys. Rev. B* **43**, 3387 (1991); B.D. Gaulin, J.N. Reimers, and T.E. Mason, *Phys. Rev. Lett.* **69** 3244 (1992).

[5] E.F. Shender, V.B. Cherepanov, P.C.W. Holdsworth, and A.J. Berlinsky, *Phys. Rev. Lett.* **70**, 3812 (1993).

[6] K. Binder and A.P. Young, *Rev. Mod. Phys.* **58**, 801 (1986).

[7] J.T. Chalker, P.C.W. Holdsworth, and E.F. Shender, *Phys. Rev. Lett.* **68**, 855 (1992).

[8] P. Chandra, P. Coleman, and I. Ritchey, *J.Phys.* **3**, 591 (1993); I. Ritchey, P. Coleman, and P. Chandra, *Phys. Rev. B* **47**, 15342 (1993).

[9] R. Liebermann, *Statistical Mechanics of Periodically Frustrated Ising Systems* (Springer-Verlag, Berlin, 1986).

[10] J.L. Leibowitz, M.K. Phani, and D.F. Styer, *J. Stat. Phys.* **38**, 413 1985.

[11] A. Gukasov, T. Brueckel, B. Dorner, V. Plakhty, W. Prandl, E. Shender, and O.P. Smirnov, *Europhys. Lett.* **7**, 83 (1988).

[12] E. Rastelli and A. Tassi, *J. Phys. C* L303 (1987); E. Rastelli, S. Sedazarri, and A. Tassi, *J. Phys. Condens. Matter* **2**, 8935 (1990).

[13] P. Chandra, P. Coleman, and A.I. Larkin, *J. Phys. Condens. Matter* **2**, 7933 (1990).

[14] A. Chubukov and T. Jolicoeur, *Phys. Rev. B* **46**, 1137 (1992).

[15] Q. Sheng and C.L. Henley, *J. Phys. Condens. Matter* **4**, 2937 (1993).

[16] O.P. Smirnov and E.F. Shender, *Sov. Phys. Sol. State* **27**, 1125 (1985).

[17] C.L. Henley, *Phys. Rev. Lett.* **62**, 2056 (1989).

[18] T. Yildirim, A.B. Harris, and E.F. Shender, *Phys. Rev. B* (to be published).

[19] R.J. Baxter, *J. Mater. Phys.* **11**, 784 (1970).

[20] A.J. Berlinsky and C. Kallin, *Hyperfine Int.* **85**, 173 (1994).

[21] C. Zeng and V. Elser, *Phys. Rev. B* **42**, 8436 (1990).

[22] A.B. Harris, C. Kallin, and A.J. Berlinsky, *Phys. Rev. B* **45**, 7536 (1992).

[23] D. Huse and A. Rutenberg, *Phys. Rev. B* **45**, 7536 (1992).

[24] J.N. Reimers and A.J. Berlinsky, preprint (1992).

[25] A. Chubukov, *Phys. Rev. Lett.* **69**, 832 (1992).

[26] V.B. Cherepanvov, personal communication, 1994.

[27] See, for example, L. Radzikhovsky and D.R. Nelson, *Phys. Rev. A* **44**, 3525 (1991).

[28] We are grateful to C.L. Henley, who attracted our attention to this fact.

[29] J. Villain, *Z.Phys. B* **33**, 31 (1989).

[30] S.T. Bramwell, M.J.P. Gingras, and J.N. Reimers, TRIUMF preprint (1993).

[31] A.P. Ramirez, private communication (1994).

[32] Ya.V. Fyodorov and E.F. Shender, *J. Phys. Condens. Matter* **3**, 9123 (1991).

[33] Y. Imry and S.K. Ma, *Phys. Rev. Lett.* **35**, 1399 (1975).

[34] D.L. Huber and W.Y. Ching, *Phys. Rev. B* **47**, 3220 (1993).

[35] J.von Delft and C.L. Henley, *Phys. Rev. Lett.* **69**, 3236 (1992); J. von Delft and C.L.Henley, *Phys. Rev. B* **48**, 965 (1993).

[36] V. Elser. *Phys. Rev. Lett.* **62**, 2405 (1990); P.W. Leung and V. Elser, *Phys. Rev. B* **47**, 5459 (1993); V. Elser and C. Zeng, preprint (1993) and references therein.

[37] B. Bernu, C. Lhuillier, and L. Pierre, *Phys. Rev. Lett.* **69**, 2590 (1992).

[38] J.T. Chalker and J.F.G. Eastmond, *Phys. Rev. B* **46**, 14201 (1992).

[39] S. Sachdev, *Phys. Rev. B* **45**, 12377 (1992).

[40] P. Chandra and B. Doucot, NEC preprint (1993).